A novel multi-antigenic parapoxvirus-based vaccine demonstrates efficacy in protecting hamsters and non-human primates against SARS-CoV-2 challenge

Alena Reguzova
University of Tübingen
Melanie Sigle
University of Tübingen
Felix Pagallies
University of Tübingen
Ferdinand Salomon
University of Tübingen
Hanns-Joachim Rziha
2University of Tuebingen, Interfaculty Institute for Cell Biology, Department of Immunology, Tuebingen
Zsofia Bittner-Schrader
University of Tübingen
Babs Verstrepen
Erasmus University Medical Center
Kinga Böszörményi
Biomedical Primate Research Centre https://orcid.org/0000-0001-5330-2617
Ernst Verschoor
Biomedical Primate Research Centre https://orcid.org/0000-0003-0912-2074
Knut Elbers
Boehringer Ingelheim GmbH
Meral Esen
University of Tübingen
Alessandro Manenti
VisMederi (Italy)
Martina Monti
VisMederi Srl. https://orcid.org/0000-0002-2173-7269
Madiha Derouazi
Speransa Therapeutics
Hans-Georg Rammensee
2University of Tuebingen, Interfaculty Institute for Cell Biology, Department of Immunology, Tuebingen
https://orcid.org/0000-0003-1614-2647

Markus Löffler (markus.loeffler@med.uni-tuebingen.de)
University of Tübingen https://orcid.org/0000-0003-2513-1317
Ralf Amann
2University of Tuebingen, Interfaculty Institute for Cell Biology, Department of Immunology, Tuebingen

Article

Keywords:

Posted Date: May 19th, 2023

DOI: https://doi.org/10.21203/rs.3.rs-2832501/v1

Abstract

The next generation of COVID-19 vaccines needs to broaden the antigenic repertoire to improve breadth of immune response and efficacy against emerging variants of concern. This study describes a new parapoxvirus-based vector (ORFV) as a platform to design a multi-antigenic vaccine targeting SARS-CoV-2 spike and nucleocapsid antigens. Two vaccine candidates were engineered, one expressing spike protein alone (ORFV-S) and the other co-expressing the more conserved nucleocapsid protein (ORFV-S/N). Both vaccines elicited comparable levels of spike-specific antibodies and virus neutralization in mice. In a SARS-CoV-2 challenge model in hamsters, the multi-antigenic ORFV-S/N vaccine conferred protection in the upper and lower respiratory tract, while the ORFV-S-vaccinated animals showed protection restricted to the lungs. Similarly, in a non-human primates challenge model, vaccination with the ORFV-S/N vaccine resulted in rapid onset and long-term protection against SARS-CoV-2 infection. These results demonstrate the potential of ORFV as a platform for prophylactic vaccination and support ongoing first-in-man studies with the multi-antigenic ORFV vaccine.

Introduction

The COVID-19 pandemic has highlighted the need for vaccine platforms enabling rapid development and manufacturing of vaccines that provide long-term protection against severe disease.

While approved COVID-19 vaccines have demonstrated high protection against severe disease, their effectiveness against (re-)infection is limited[1] and transient due to waning immunity over time.[2] Additionally, SARS-CoV-2 Variants of Concern (VoC) with constantly accumulating mutations represent a challenge for current vaccines.[1] To address this challenge, next-generation vaccines need to stimulate broader humoral and cellular immunity by incorporating several immunodominant antigens.[3, 4, 5, 6]

Addressing the well-conserved nucleocapsid protein as a promising target antigen in addition to the spike protein may improve vaccine efficacy.[7, 8, 9, 10, 11, 12] Incorporating the nucleocapsid protein could substantially increase cell-mediated immunity[7] and facilitate cross-reactive T cell responses. This strategy may enable protection independent of the constantly mutating spike protein[13] thereby circumventing the challenge posed by future SARS-CoV-2 variants.[8] Currently, various approaches targeting nucleocapsid protein have been evaluated preclinically[14, 15, 16, 17, 18, 19, 20, 21] or are already in clinical development[22] (ClinicalTrials.gov Identifier: NCT04732468; NCT04546841; NCT04639466 and NCT04977024; NCT05370040).

This study reports on a novel vaccine platform based on the Orf virus strain D1701-VrV (ORFV), a member of the genus *Parapoxvirus.* This platform is specifically designed to support multi-antigenic vaccine concepts. Unlike the majority of viral vectors, ORFV allows effective re-immunizations due to short-lived vector-specific immunity, along with the induction of robust and long-lasting immune responses to vector-encoded antigens.[23, 24, 25, 26, 27, 28, 29, 30] Using the ORFV vector platform, we engineered two COVID-19 vaccine candidates expressing either the stabilized full-length spike protein

alone (ORFV-S, mono-antigenic) or co-expressing nucleocapsid protein (ORFV-S/N, multi-antigenic). We monitored humoral and cellular immunity in naïve mice, as well as in SARS-CoV-2 challenge models in hamsters and non-human primates (NHPs). In mice, ORFV-S and ORFV-S/N vaccines both induced comparable increases in anti-spike humoral and cellular immune responses. After a single vaccination with the ORFV-S/N vaccine, complete protection against SARS-CoV-2 in the upper and lower airways was achieved in hamsters. Moreover, we confirmed strong and long-lasting immunity along with protection against SARS-CoV-2 infection in NHPs vaccinated with the same multi-antigenic ORFV-S/N vaccine. These results provide the basis for two ongoing phase 1 clinical studies assessing safety and dosing for a multi-antigenic ORFV-based vaccine (NCT05367843 and NCT05389319).

Results

Construction of ORFV D1701-VrV-based SARS-CoV-2 recombinants expressing spike protein alone or in combination with nucleocapsid protein

We used the D1701-VrV ORFV vector[31, 32] to generate two SARS-CoV-2 vaccine candidates as described previously (Fig. 1A).[26] The full-length spike protein from of the ancestral SARS-CoV-2 (Wuhan) genomic sequence[33] was inserted into the *vegf-e* locus under the control of the early *Pvegf* promotor of D1701-VrV ORFV in both recombinants. The spike protein sequence included mutations D614G, mutation K986P and V987P for proline stabilization and a furin cleavage site deletion (aa 682–685 RRAR to GSAS.)[34] The nucleocapsid gene was inserted in the D (*Del2)* locus under control of an artificial early *P7* promotor, generating a double transgene-containing recombinant (ORFV-S/N) (Fig. 1A). The early *Pvegf* and P7 promotors initiated antigen expression encoded in the virus in the cytoplasm of the infected cells. We confirmed the integrity, correct and stable insertion of transgenes by vegf-, Del2- and transgene-specific PCR, and gene sequencing. We used an empty D1701-VrV ORFV vector as a control (ORFV-Mock).

We confirmed spike protein expression from ORFV-S and ORFV-S/N by flow cytometry 20 hours after infecting Vero cells using multiplicity of infection (MOI) of 1 by cell surface staining (Fig. 1B; left panel) and intracellular staining (Fig. 1B; middle panel). The mean fluorescence intensities were comparable for both recombinants. We also verified intracellular nucleocapsid protein production by flow cytometry in Vero cells infected with the ORFV-S/N recombinant (Fig. 1B; right panel) and confirmed the correct transgene expression by western blotting using Vero cells harvested 48 hours after infection (MOI 1) and detected specific bands (180 kDa) in cell lysates using antibodies against S1 and S2 subunits of spike protein (Fig. 1C), as well as against the nucleocapsid protein (46 kDa) (Fig. 1C).

Mono- and multi-antigenic ORFV recombinants induce robust and long-lasting T_H 1-biased antibody- and cellular immune responses against inserted transgenes in mice

The immunogenicity of both ORFV-based vaccine candidates was evaluated in CD-1 mice after two intramuscular (i.m.) injections with a 21-days interval using 10^7 PFU. Mice immunized with ORFV-Mock recombinant were used as controls (Fig. 2A). After a single injection, both ORFV vaccines induced similar

levels of RBD-specific binding antibodies with geometric mean endpoint titers (GMT) of 3.9×10^5 and 2.3×10^5, respectively, 3-weeks after vaccination (Fig. 2B). A second dose of either ORFV-S or ORFV-S/N increased the antigen-specific binding antibody titers at day 28 by 1.9- and 3.4-fold, respectively. The IgG2a/IgG1 isotype ratio of RBD-binding antibodies at day 28 showed a T_H1-biased profile skewed towards IgG2a for both ORFV-S and ORFV-S/N (Fig. 2C). Virus neutralizing titers (VNT) were similar for both constructs, with a GMT of 2.0×10^3 and 1.7×10^3 for ORFV-S and ORFV-S/N, respectively, compared to 4.5×10^2 with the WHO International Standard of anti-SARS-CoV-2 immunoglobulin NIBSC 20/136 (Fig. 2D).

The ORFV-S/N also induced a robust antibody response to the nucleocapsid, which was significantly boosted after the second vaccination (Fig. 1E). The specific IgG2a/IgG1 ratios confirmed a T_H1 profile after ORFV-S/N immunization (Fig. 1F).

In addition to the humoral immune response, both ORFV-S and ORFV-S/N recombinants elicited multifunctional CD4 + and CD8 + T cells specific for spike (Fig. 1G, S1A, S1C) and nucleocapsid (Fig. 1H, S1A, S1B), as monitored in spleens seven days after the second vaccination.

The long-term persistence of the vaccine-induced humoral responses as well as boost capacity of the ORFV-based SARS-CoV-2 vaccine candidates was further assessed in mice (Fig. S2A). ORFV-S and ORFV-S/N recombinants elicited elevated RBD-binding total IgG levels over the prolonged follow-up period, and a third vaccination (day 171) boosted pre-existing antibody levels by 2.2- and 1.5-fold for ORFV-S and ORFV-S/N, respectively (Fig. S2B). The antibody levels against nucleocapsid were boosted by 44.6-fold following the third vaccination using ORFV-S/N (Fig. S2C). VNT after the second (day 35) and the third vaccination (day 185) for both ORFV-S and ORFV-S/N were similar (Fig. S2D).

Multi-antigenic ORFV-S/N recombinant confers superior protection to vaccinated Syrian hamsters following SARS-CoV-2 challenge as compared to the mono-antigenic ORFV-S

The Syrian hamster SARS-CoV-2 challenge model is a well-established system to study severe COVID-19 with pathology similar to humans[35]. In this study, hamsters were vaccinated twice at a 4-week interval with either escalating doses (10^6 – 10^8 PFU) or a single dose of the highest dose (10^8 PFU) of the ORFV-S/N recombinant, or two doses (10^7 PFU) of ORFV-S recombinant or PBS. In addition, a group of hamsters was infected with SARS-CoV-2 (10^2 $TCID_{50}$ intranasally) (ancestral strain; Wuhan) at day 0 (SARS-CoV-2-recovered). All animals were challenged with SARS-CoV-2 (10^2 $TCID_{50}$) (ancestral strain; Wuhan) at day 56 (Fig. 3A).

After the first and second vaccination, a dose-dependent increase of RBD-binding IgG antibodies was observed in all groups (Fig. 3B). A correlation was also observed between total antibody levels and VNT.

Four days after SARS-CoV-2 challenge, virus titers were assessed in the nose and lungs, along with lung histopathology. Hamsters vaccinated with ORFV-S and ORFV-S/N and those recovered from a previous

SARS-CoV-2 infection showed reduced virus titers in the lungs (Fig. 3D). However, only ORFV-S/N vaccine consistently prevented the presence of virus in the upper respiratory tracts, despite lower antibody and VNT (Fig. 3E).

Histopathological evaluations showed that the ORFV-S/N vaccine conferred protection with minimal affection of the upper and lower airways (Fig. 3F). Vaccination with ORFV-S/N doses at 10^7 and 10^8 PFU resulted in the lowest scores of rhinitis, tracheitis, bronchiolitis and alveolitis, whereas two doses of 10^6 PFU or a single dose of 10^8 PFU of ORFV-S/N already reduced severity of rhinitis and tracheitis. Interestingly, the ORFV-S recombinant did not protect the vaccinated hamsters from severe rhinitis with scores comparable to the PBS group. However, the histopathology scores of tracheitis and alveolitis were clearly reduced when compared to the PBS group (Fig. 3F). SARS-CoV-2-recovered animals showed increased scores of rhinitis, tracheitis and alveolitis as compared to animals vaccinated with ORFV-S/N, although the scores were lower than those found in the PBS group.

Correlates of protection analyses showed that high VNT elicited by the ORFV-S recombinant did not cluster with reduced viral titers in nasal turbinates, in contrast to the effects observed after one or two administrations of ORFV-S/N. The latter elicited better protection against viral challenge that included the upper airways (Fig. 3G). In addition, no correlation was observed between the VNT after vaccination with both ORFV-S and ORFV-S/N recombinants and the elevated virus titers in lungs after the challenge (Fig. 3H). Clustering of higher VNT levels with reduced histopathology scores suggested possible vaccine dose-dependent effects (Fig. 3I).

The potential of both ORFV-S and ORFV-S/N vaccine candidates to boost pre-existing memory responses after SARS-CoV-2 infection was also investigated in the hamster model. Animals were infected with SARS-CoV-2 (10^2 $TCID_{50}$ intranasally) (SARS-CoV-2-recovered) and 42 days later either vaccinated with $3x10^7$ PFU of ORFV-S and ORFV-S/N, or re-infected with SARS-CoV-2. Hamsters were monitored until day 56 (Fig. S3A). Already seven days after the boost with either ORFV-S or ORFV-S/N (day 49), increased RBD-binding IgG titers were observed (Fig. S3B; Table S1). Administration of ORFV-S or ORFV-S/N resulted in 4.5- or 2.6-fold higher RBD-specific antibody levels when compared to re-infection, respectively. Additionally, both vaccinations with the ORFV-S/N recombinant as well as the SARS-CoV-2 re-challenge boosted nucleocapsid-specific antibody levels (Fig. S3C; Table S2). Finally, administration of ORFV-S or ORFV-S/N after SARS-CoV-2 infection increased VNT by 3.6- and 3.5-fold as compared to re-infection, respectively (Fig. S3D; Table S3).

Multi-antigenic ORFV-S/N recombinant protects vaccinated non-human primates from SARS-CoV-2 infection

The superior protection observed in the Syrian hamster model following SARS-CoV-2 challenge prompted an evaluation of ORFV-S/N in a NHP challenge model. NHPs received either two doses of 10^8 PFU of the ORFV-S/N recombinant with a 4-week interval or PBS as a control (Fig. 4A). Serum and peripheral blood

mononuclear cells (PBMCs) were sampled regularly, and animals were challenged with 10^5 $TCID_{50}$ SARS-CoV-2, administered into nose and trachea on day 70. Subsequently, SARS-CoV-2 subgenomic messenger RNA (CoVsg) levels were determined daily in nose and throat over one week, and viral titers in bronchoalveolar lavage (BAL) were assessed on day 3 following challenge.

RBD-binding IgG became detectable within 14 days after the first vaccination reaching GMT of 5.0×10^4 (Fig. 4B). The second vaccination boosted antibody titers by a 9-fold 2 weeks post vaccination. Levels of spike-trimer-binding total IgG and VNT exhibited similar response patterns (Fig. 4C, D). Before challenge, RBD-binding IgG, spike-trimer-binding IgG and neutralizing GMT accounted for 1.4×10^4, 5.0×10^4 and 3.4×10^2, respectively. These values remained at baseline in the PBS group. Antibody levels against nucleocapsid protein stayed at baseline. Both, nucleocapsid- and spike-specific T cell responses with a mean of 69 and 541 IFN-γ spot forming units, respectively, were measured in PBMCs at day 35 by ELISpot (Fig. 4E).

After challenge with 10^5 $TCID_{50}$ SARS-CoV-2, half of the vaccinated animals showed detectable viral titers in nose and throat (3/6), and all cleared the virus already at day 4 in contrast to the PBS control group that remained viremic for at least one week (Fig. 4F, G). Viral loads in CoVsg PCR-positive primates were 10- to 100-times lower than in the macaques that received PBS (control). None of the vaccinated NHP showed presence of viral titers in BAL, in contrast to all animals in the control group (Fig. 4H).

To evaluate the duration of ORFV-mediated vaccine protection, NHP were first vaccinated with the ORFV-S/N at a dose of 10^6 or $3x10^7$ PFU or PBS as a control with a 4-week interval, and then challenged with 10^5 $TCID_{50}$ of SARS-CoV-2 seventeen weeks after the last vaccination (Fig. S4). In this long-term experiment, viral loads in CoVsg PCR-positive primates were 2- to 150-times lower than in the macaques that had received PBS (control). In addition, 80% of NHP immunized with the $3x10^7$ PFU of ORFV-S/N recombinant still showed protection against SARS-CoV-2 in the lungs.

Discussion

The emergence of new SARS-CoV-2 variants[1] and the waning antibody levels[36, 37, 38, 39, 40, 41] and protection over time[2] as well as continuously emerging SARS-CoV-2 virus variants[1] demand further development of innovative vaccine technologies. Broadening SARS-CoV-2-specific humoral and cellular immunity by incorporating multiple viral antigens into vaccines, or the use of heterologous vaccination approaches are promising strategies that can improve vaccine-induced immune responses and avoid potential challenges with antigenic imprinting with mutated SARS-CoV-2 VoC.[42] In this context, the highly conserved nucleocapsid protein, in addition to the spike protein, holds promise as an attractive antigen that can provide durable and broadly reactive T cells, thereby enhancing protection against VoC.[8]

To investigate such a multi-antigenic vaccination approach against COVID-19, a novel versatile parapoxviral vector platform based on the attenuated Orf virus strain ORFV D1701-VrV[26, 31, 43] was used

to develop vaccine candidates expressing the stabilized full-length spike protein alone or together with the nucleocapsid protein. Both mono- and multi-antigenic ORFV-vaccine candidates induced immunity for at least 5 months in mice, with comparable high spike binding and virus-neutralizing antibody titers after two vaccinations.

Cross-reactive T cells are considered instrumental in maintaining immunity against VoC, especially in cases of humoral immune escape.[44, 45] Recently, a potential role of vaccine-induced CD8 + T cells in protecting against Omicron VoC challenge elicited by a mRNA vaccine encoding the full-length spike and nucleocapsid proteins of the ancestral SARS-CoV-2 strain (mRNA-S + N) was shown in a hamster model.[14] Accordingly, the ORFV-S/N vaccination approach triggered a T_H1-biased immune responses and induced multifunctional target-specific CD8 + and CD4 + T cells. In the context of a booster vaccination in mice with pre-existing humoral immune responses, the ORFV-S/N recombinant resulted in higher SARS-CoV-2 antibody binding- and virus neutralizing titers than the S ORFV recombinant, which was potentially mediated via improved CD4 + T cell help.[46]

With its high genetic similarity to the human ACE2 receptor[47], the golden Syrian hamster model is state-of-the-art for investigating protection against SARS-CoV-2 challenge. In hamsters, only the ORFV-S/N vaccine led to rapid virus clearance in the upper respiratory tract and lungs starting 4 days after virus challenge and enabling complete protection, whereas the protective effects of the ORFV-S vaccine remained restricted to the lower airways (lungs) despite higher RBD-binding antibody levels. Similar observations were recently made following challenge of mRNA-S + N vaccinated hamsters with SARS-CoV-2 Delta and Omicron VoC.[14] These findings suggest that nucleocapsid-mediated immune responses may relevantly contribute to full protection and that the levels of neutralizing antibodies are not necessarily the only correlate of vaccine efficacy. However, vaccines targeting nucleocapsid alone have been established as ineffective[18] or provide only very modest protection against SARS-CoV-2[14] indicating that multi-antigenic vaccination is a more promising approach.

The ORFV-S/N vaccine candidate was also shown to be effective for boosting broad pre-existing memory responses after SARS-CoV-2 infection. Vaccination following a SARS-CoV-2 infection elicited high titers of spike-binding antibodies and potent virus neutralization capacity as well as a more consistent increase of nucleocapsid-binding IgG levels in hamsters, when compared to re-infection. Considering that a large part of the global population meanwhile has been infected with SARS-CoV-2, these findings support the potential of the ORFV-S/N vaccine candidate as an effective booster against COVID-19.

The ORFV-S/N lead vaccine candidate was evaluated in the well-established pre-clinical NHP challenge model. After vaccination with the ORFV-S/N vaccine, rhesus macaques developed humoral immune responses and T cells specific for both the spike- and nucleocapsid protein after two injections. Following SARS-CoV-2 infection, vaccinated animals showed rapid virus clearance in the nose and throat and no detectable virus in bronchoalveolar lavage, suggesting that the SARSCoV-2 virus remained restricted to the upper airways and did not affect the lungs. The durability of protection against SARS-CoV-2 was

further confirmed in a long-term experiment, where two vaccinations with the ORFV-S/N recombinant conferred protection of the lungs after 5 months in 80% of NHP.

In conclusion, the presented results highlight the potential of ORFV as a novel vaccine platform and suggest that immune responses against nucleocapsid can help to broaden immune responses and improve immunity against SARS-CoV-2 VoC.[14] Two ongoing multicenter Phase I clinical trials are evaluating the multi-antigenic ORFV-S/N lead vaccine candidate (ClinicalTrials.gov identifier: NCT05389319 and NCT05367843) and shall provide additional information on the safety, reactogenicity, immunogenicity and suitability for a heterologous boost approach in human.

Methods

Study Design

This study was designed to evaluate the immunogenicity and protective efficacy of ORFV-based vaccine candidates against SARS-CoV-2, containing the spike protein alone or in combination with nucleocapsid protein. Transgene expression was validated in cell culture by flow cytometry and Western blotting. Preclinical assessments were conducted in rodents and cynomolgus macaques. For *in vitro* and *in vivo* assays, sample sizes were calculated by the investigators on the basis of previous experience or suitable publications. All *in vitro* studies were performed at least twice with highly comparable outcomes.

Ethics statement and experimental models

Mice

Male and female CD-1 mice were purchased and handled in strict accordance to Federation of European Laboratory Animal Science Associations (FELASA) recommendations and followed the guidelines of the Regional councils. Experiments were carried out at the biosafety level 1 (BSL1) animal facility at the University of Tübingen, Germany under the Project License Nr. IM1/20G.

Hamsters

Syrian golden hamsters were purchased and all experiments were carried out under BSL3 conditions at Viroclinics Xplore animal facility (Schaijk, The Netherlands) under the Project License Nr. 27700202114492-WP02. All animals were treated with strict accordance with Dutch law for animal experimentation and Directive 2010/63/EU of the European Parliament and of the Council of 22 September 2010 on the protection of animals used for scientific purposes.

Macaques

Rhesus macaques (*Macaca mulatta*) were mature, outbred animals, purpose-bred and housed at the Biomedical Primate Research Centre (BPRC) (Rijswijk, The Netherlands). Experiments were carried out under BSL3 + conditions under the Project License Nr. CCD 028H. The study was reviewed and approved

by the Dutch “Centrale Commissie Dierproeven” (AVD5020020209404) according to Dutch law, article 10a of the “Wet op de Dierproeven” and BPRC’s Animal Welfare Body (IvD).

Generation of D1701-VrV-based SARS-CoV-2 ORFV recombinants

The SARS-CoV-2 spike and nucleocapsid protein genes were synthesized by Gene Art (Thermo Fisher Scientific, Waltham, MA, USA). The spike gene was cloned into plasmid pV12-Cherry; the nucleocapsid gene was cloned into plasmid pD12-Cherry.[26] Correct insertions and sequences were verified by restriction digestion and sequencing (Eurofins Genomics, Ebersberg, Germany). The resulting transfer plasmids were used for transfection of Vero E6 cells (cat. no. CRL-1586, American Type Culture Collection (ATCC), Manassas, VA, USA) infected with D1701-VrV-V12-Cherry using SF Cell Line 4D-Nucleofector™ X Kit (Lonza, Köln, Germany) to replace the encoded Cherry gene by homologous recombination as described previously.[26, 43] Transfer plasmids pV-CoV-Spike and pD7-CoV-N were used to transfect Vero cells infected with D1701-VrV-GFP-D12-Cherry to replace GFP and Cherry genes, respectively. The new ORFV recombinants D1701-VrV-CoV-Spike and D1701-VrV-CoV-Spike-D7-CoV-N were selected by fluorescence-activated cell sorting using a SH800S Cell Sorter (Sony Biotechnology, Bothell, WA, USA). Identification of ORFV recombinants was accomplished by polymerase chain reaction (PCR) using insert- and locus-specific primers. ORFV recombinants were propagated and purified as described previously.[43] Ten serial passages were performed in Vero cells to track the genetic stability of the inserted proteins. Virus titers were determined by a standard plaque assay.[26]

In vitro **transgene expression**

Vero cells were seeded into 6-well plates (Greiner Bio-One, Frickenhausen, Germany) at a density of 5×10^5 cells/well and infected with ORFV recombinants at a multiplicity of infection (MOI) of 1. For flow cytometry, protein expression was assessed 24 h post infection. Cell surface staining was performed with SARS-CoV-2 Spike Neutralizing Antibody (cat. no. 40592-R001, Sino Biological, Eschborn, Germany) and anti-ORFV antibody (produced in-house), cells were fixed using Fixation & Permeabilization Solution (BD Biosciences, Franklin Lakes, NJ, USA) followed by intracellular staining with SARS-CoV-2 nucleocapsid antibody (cat. no. GTX135357, GeneTex, Irvine, CA, USA). Cells were acquired on a BD LSR Fortessa (BD Biosciences) and analyzed using the FlowJo® software (BD Biosciences). For Western blotting, supernatants obtained 48 h post infection were collected and cells were lysed in radioimmunoprecipitation assay (RIPA) lysis buffer containing protease/phosphatase inhibitors (Sigma-Aldrich, St. Louis, MO, USA). Cleared cell lysates were used for standard SDS-PAGE followed by immunoblot using SARS-CoV-2 spike neutralizing (anti-S1) (cat. no. 40592-R001, Sino Biological), spike (anti-S2) (cat. no. GTX632604, GeneTex), and nucleocapsid antibodies (cat. no. GTX135357, GeneTex). Anti-ORFV antibody (produced in-house) was used as a loading control. Fusion FL camera and FusionCapt Advance software (PEQLAB, Erlangen, Germany) were used for membrane exposure.

Animal immunization and challenge experiments

Mice

CD-1 mice (Charles River Laboratories, Sulzfeld, Germany) were immunized intramuscularly (i.m.) at day 0 and 21 with ORFV-Mock, or ORFV-S or ORFV-S/N recombinants. For extended study, a third immunization was done on day 171. Alternatively, different ORFV-S/N doses were administered on days 0, 21 and 171, or on days 0 and 171 only. Blood was collected on days 21, 28, 171 and 185. Upon euthanasia splenocytes were isolated utilizing standard procedures initially from five mice per group on days 28 and from the remainder of mice on day 171.

Hamsters

Syrian golden hamsters (Janvier, Le Genest-Saint-Isle, France) were immunized i.m. with ORFV-S/N or ORFV-S recombinants at day 0 and 28 or with ORFV-S/N on day 28 only. PBS was injected at day 0 and 28 as a negative control. For comparison, hamsters were infected intranasally (i.n.) on day 0 with 10^2 $TCID_{50}$/dose of SARS-CoV-2 EU isolate BetaCoV/Munich/BavPat1/2020 (ancestral strain; Wuhan). Blood samples were collected on days 0, 28, 42 and 56. All animals were challenged with SARS-CoV-2 (ancestral strain; Wuhan) on day 56, administered as above. Four days after challenge, swabs of respiratory tract were sampled, hamsters were euthanized and tissue samples were obtained for analysis. For the study evaluating boosting effects of ORFV recombinants in SARS-CoV-2 experienced hamsters, animals were infected i.n. with SARS-CoV-2 (ancestral strain; Wuhan) as described above on day 0 and boosted with ORFV-S/N or ORFV-S recombinants on day 42. For comparison, hamsters were challenged with SARS-CoV-2 (ancestral strain; Wuhan) at day 42. Blood was collected on days 0, 21, 42, 49 and 56.

Macaques

Rhesus macaques (*Macaca mulatta*) were immunized i.m. at day 0 and 28 with ORFV-S/N recombinant or PBS. Blood was obtained on days 0, 14, 28, 42 and 70, and PBMC on days 7 and 35. Macaques were challenged on day 70 with 10^5 $TCID_{50}$/dose of SARS-CoV-2 strain BetaCoV/German/BavPat1/2020 (ancestral strain; Wuhan-type) via a combined intranasal/intratracheal route. For the extended study, macaques were immunized i.m. at day 0 and 28 with different doses of ORFV-S/N recombinant or PBS. Serum was obtained on days 0, 14, 28, 42 and 147, and PBMC on days 7 and 35. Animals were challenged on day 147 as described above. All macaques from both studies were monitored for SARS-CoV-2-related disease symptoms for the next 7–10 days. Tracheal and nasal swabs were collected daily after SARS-CoV-2 exposure, bronchoalveolar lavage (BAL) was obtained 3 days post challenge.

Detection of specific serum IgG

SARS-CoV-2-specific antibody titers were determined using SARS-CoV-2 S1 RBD- (IEQ-CoVS1RBD-IgG-5) and N-protein ELISA kit (IEQ-CoVN-IgG) (both Ray Biotech, Peachtree Corners, GA, USA) or SARS-CoV-2 Spike Trimer ELISA kit (Invitrogen, Carlsbad, CA, USA, BMS2324TEN). For detection of ORFV-binding antibodies, Nunc Maxisorp 96-well cell plates (Fisher Scientific, Schwerte, Germany) were coated with 5×10^5 PFU of ORFV D1701-VrV at 4° C overnight followed by 2 h blocking using 3% of bovine serum albumin. HRP-conjugated secondary antibodies were used to detect total bound IgG (1:5000, ab6728),

IgG1 (1:1000, ab97240,) and IgG2a (1:1000, ab97245) subclasses in mouse serum, total bound IgG in hamster serum (1:10000, ab6892) and in NHP serum (1:10000, ab112767) (all Abcam, Cambridge, UK). All serum samples and controls were evaluated in duplicates. Blank absorbance units (OD) values were subtracted from the average values of sample duplicates. For calculation of the endpoint titer, the log10 OD values of the samples were plotted against the log10 of the sample dilution, and a regression analysis was performed. As a cut-off OD = 0.1 was used and endpoint titer was defined as the value where the linear regression line of the cut-off intercepted with the regression line of the samples. WHO International Reference Panel with high levels of anti-SARS-CoV-2 immunoglobulin (NIBSC 20/150) was used as a standard.

SARS-CoV-2 Virus Neutralization Test

Analyses samples from hamsters were done at Viroclinics Xplore (Schaijk, The Netherlands), NHP samples at Wageningen Bioveterinary Research (Lelystad, The Netherlands). Sera were heat inactivated for 30 min at 56° C. Sample dilutions in triplicates were incubated with 10^2 $TCID_{50}$/well of SARS-CoV-2 (ancestral strain; Wuhan) for 1 h at 37° C (hamster) or in duplicates for 1.5 h at room temperature (macaques). Vero E6 cells (ATCC, CRL-1586) were added to the wells. Plates containing hamster serum were incubated for 5–6 days and scored for the presence of cytopathogenic effects (CPE) (100% end point) using a water-soluble tetrazolium salt (WST-8 cell proliferation assay; Promocell, Heidelberg, Germany). Virus neutralization titers (VNT) were calculated according to the method described by Reed & Muench.[48] For macaques' samples, plates were incubated for 6–7 days. The virus neutralizing titer was determined either microscopically or through an Immuno Peroxidase Monolayer Assay (IPMA) staining as the reciprocal dilution at which CPE reached 50%. WHO International Standard for anti-SARS-CoV-2 immunoglobulin (NIBSC 20/136) was used as a reference, where indicated.

Intracellular cytokine staining (ICS)

Freshly isolated mouse splenocytes were seeded into a 96-well plate (Greiner Bio-One) at a density of 2 x 10^6 cells/well and re-stimulated using 0.5 µg/mL of SARS-CoV-2 full-length spike- (PM-WCPV-S-1) or nucleocapsid peptide libraries (PM-WCPV-NCAP-1) (all JPT Peptide Technologies, Berlin, Germany) and 1 µg/mL of co-stimulatory anti-mouse CD28 (cat. no. 102116) and CD49d (cat. no. 103710) antibodies (all BioLegend, San Diego, CA, USA). After 1 h, 10 µg/mL of Brefeldin A (Sigma-Aldrich, St. Louis, MO, USA) was added for 14 h. Cells were first treated for 10 min with TruStain FcX™ (cat. no. 101320, BioLegend). Afterwards anti-mouse surface antibody cocktail was added for 30 min into the wells, containing CD3ε (cat. no. 100312), CD4 (cat. no. 100531), CD8a (cat. no. 100730), CD62L (cat. no. 104430) and CD44 (cat. no. 103022) antibodies in combination with Zombie Aqua Fixable viability dye (cat. no. 423102) (all BioLegend). Cells were further permeabilized for 30 min using Fixation & Permeabilization Solution (BD Bioscience) and incubated for 30 min with anti-mouse TNF (cat. no. 506324), IFN-γ (cat. no. 505835) and IL-2 (cat. no. 503808) antibody-mix (all BioLegend). Cells were acquired on a BD LSR Fortessa and analyzed using the FlowJo® software. The background in unstimulated wells was subtracted from the peptide-stimulated wells.

IFN-γ ELISpot assay

Cryopreserved PBMCs of macaques were thawed by standard procedure. Assays were performed in triplicates using Monkey IFN-γ ELISpot PLUS (ALP) kit (Mabtech, Stockholm, Sweden). Plates were blocked for 30 min with CTS OpTmizer medium (Gibco, Fisher Scientific) and 1 µg/mL of SARS-CoV-2 full-length spike- (PM-WCPV-S-1) or nucleocapsid peptide libraries (PM-WCPV-NCAP-1) (all JPT Peptide Technologies) in CTS OpTmizer medium was added into the wells. Next, 1–2 x 10^5 cells were seeded into each well with *stimuli* and incubated for 20 h. Spots were counted on ImmunoSpot S6 Universal Analyzer CTL reader (Cellular Technology Limited, Shaker Heights, OH, USA). Mean of the triplicates was calculated and background in unstimulated wells was subtracted. Spot numbers were normalized to 1 x 10^6 cells for each sample.

Viral load in the respiratory tract

Detection of replication competent SARS-CoV-2 virus in hamster nasal turbinate tissues, throat swabs and lungs post challenge was performed at Viroclinics Xplore (Schaijk, The Netherlands). Briefly, sample serial dilutions were transferred in quadruplicates into 96-well plates (Greiner Bio-One), containing Vero E6 cell monolayers and incubated for 1 h at 37° C. Afterwards, cells were washed and incubated for 5 days. Plates were scored using WST-8 marker (Promocell) and viral titers (Log10 $TCID_{50}$/ml or /g) were calculated using the Spearman-Karber's method.

Viral loads in the respiratory tract of challenged macaques were assessed at the Biomedical Primate Research Centre, The Netherlands. Briefly, SARS-CoV-2 genomic RNA was determined by real-time quantitative RT-PCR as described by Corman et al.[49], a sub-genomic (sgm) RT-qPCR was performed as described by Wölfel[50] and Perera[51]. Viral RNA extractions were done using the QIAamp® Viral RNA Mini Kit (Qiagen, Hilden, Germany). The cDNA synthesis and PCR amplification were performed using the Brilliant II qRT-PCR Core Reagent Kit, 1-Step kit (Agilent, Santa Clara, CA, USA), and RNA was quantified on a Bio-Rad CFX Connect real-time system (Bio-Rad Laboratories GmbH, Feldkirchen, Germany).

Histopathology

Histopathological analysis of respiratory tract tissues was conducted for hamsters euthanised due to reaching experimental endpoint (day 60). After fixation with 10% formalin, tissue sections were embedded in paraffin and stained with hematoxylin and eosin. Histopathological assessment of stained slides was performed by a certified veterinary pathologist at the Department of Pathology, University of Veterinary Medicine (Hannover, Germany). Histopathological severity assessment scoring is as follows: 0 = no inflammatory cells, 1 = a few inflammatory cells, 2 = moderate numbers of inflammatory cells, 3 = many inflammatory cells.

Quantification and statistical analysis

Data were processed and analyzed with GraphPad Prism 9 software (GraphPad, San Diego, CA). Where applicable the distributions of variables were assessed using Shapiro-Wilk test of normality. Normally

distributed variables among multiple groups were compared by one-way analysis of variance (ANOVA) with Bonferroni correction for multiple comparisons. Otherwise, Kruskal-Wallis test was used. Data were presented as the means ± SEM or as geometric mean with geometric SD. P values < 0.05 were considered statistically significant. Significance is annotated with respective symbols (* $p < 0.05$; ** $p < 0.01$; *** $p < 0.001$).

Data availability

All relevant data generated or analyzed during this study are included in this published article and its supplementary information files.

Material availability

Further information and requests for resources and reagents should be directed to and will be fulfilled with a completed Materials Transfer Agreement by the corresponding author, Ralf Amann (ralf.amann@ifiz.uni-tuebingen.de). All unique materials generated in this study are available from the corresponding author upon request.

Declarations

Data availability

All relevant data generated or analyzed during this study are included in this published article and its supplementary information files.

Material availability

Further information and requests for resources and reagents should be directed to and will be fulfilled with a completed Materials Transfer Agreement by the corresponding author, Ralf Amann (ralf.amann@ifiz.uni-tuebingen.de). All unique materials generated in this study are available from the corresponding author upon request.

Acknowledgements

We thank Anne Mohrholz, Petra Schwarzmaier and Malgorzata Wronska for excellent laboratory technical assistance. We acknowledge employees of Viroclinics Xplore for performing animal studies. We thank Mirriam Tacken and members of Department of Virology, Wageningen Bioveterinary Research for performing SARS-CoV-2 virus neutralization test.

Funding

This research was supported in part by the EXIST Forschungstransfer of the German Ministry for Economic Affairs and Energy, which is co-financed by the European Social Fund and the Carl Zeiss Stiftung. We acknowledge support by Open Access Publishing Fund of the University of Tübingen.

Author Contributions

Conceptualization: R.A., B.E.V, E.J.V., H-G.R., K.E., H-J. R., M.D., M.E.

Methodology: A.R., M.S., F.P, Z.B-S, R.A., B.E.V., K.P.B., M.M., A.M.

Investigation: A.R., M.S., F.P, Z.B-S, R.A., B.E.V., K.P.B., A.M.

Visualization: A.R., M.S., Z.B-S, F.S., R.A., M.W.L., A.M.

Funding acquisition: R.A., F.S.

Project administration: R.A., A.R., M.M.

Supervision: R.A., B.E.V, E.J.V., K.E., H-J.R., M.D., M.E., H-G. R., M.M.

Writing – original draft: A.R., M.W.L.

Writing – review & editing: R.A., B.E.V, E.J.V., K.E., M.D., M.E., H-G. R., H-J.R.

Competing interests

R.A., M.S. and F.S. have ownership interest in Prime Vector Technologies GmbH. R.A. is an inventor of patents on ORFV. M.W.L. is an inventor of patents owned by Immatics Biotechnologies unrelated to this present work and has acted as a paid consultant in cancer immunology for Boehringer Ingelheim. M.M. and A.M. are employees of VisMederi Srl. The remaining authors declare that the research was conducted in the absence of any commercial or financial relationships that could be construed as a potential conflict of interest.

References

1. Feikin, D.R. *et al.* Duration of effectiveness of vaccines against SARS-CoV-2 infection and COVID-19 disease: results of a systematic review and meta-regression. Lancet 399, 924–944 (2022).
2. Townsend, J.P., Hassler, H.B., Sah, P., Galvani, A.P. & Dornburg, A. The durability of natural infection and vaccine-induced immunity against future infection by SARS-CoV-2. Proc Natl Acad Sci U S A 119, e2204336119 (2022).
3. Wuertz, K.M. *et al.* A SARS-CoV-2 spike ferritin nanoparticle vaccine protects hamsters against Alpha and Beta virus variant challenge. NPJ Vaccines 6, 129 (2021).
4. Naranbhai, V. *et al.* T cell reactivity to the SARS-CoV-2 Omicron variant is preserved in most but not all individuals. Cell 185, 1259 (2022).
5. Geers, D. *et al.* SARS-CoV-2 variants of concern partially escape humoral but not T-cell responses in COVID-19 convalescent donors and vaccinees. Sci Immunol 6 (2021).

6. Ni, L. *et al.* Detection of SARS-CoV-2-Specific Humoral and Cellular Immunity in COVID-19 Convalescent Individuals. Immunity 52, 971–977 e973 (2020).
7. Oronsky, B. *et al.* Nucleocapsid as a next-generation COVID-19 vaccine candidate. Int J Infect Dis 122, 529–530 (2022).
8. Dutta, N.K., Mazumdar, K. & Gordy, J.T. The Nucleocapsid Protein of SARS-CoV-2: a Target for Vaccine Development. J Virol 94 (2020).
9. Thura, M. *et al.* Targeting intra-viral conserved nucleocapsid (N) proteins as novel vaccines against SARS-CoVs. Biosci Rep 41 (2021).
10. Chang, C.K., Hou, M.H., Chang, C.F., Hsiao, C.D. & Huang, T.H. The SARS coronavirus nucleocapsid protein–forms and functions. Antiviral Res 103, 39–50 (2014).
11. de Breyne, S. *et al.* Translational control of coronaviruses. Nucleic Acids Res 48, 12502–12522 (2020).
12. Weiss, S.R. & Leibowitz, J.L. Coronavirus pathogenesis. Adv Virus Res 81, 85–164 (2011).
13. Matchett, W.E. *et al.* Cutting Edge: Nucleocapsid Vaccine Elicits Spike-Independent SARS-CoV-2 Protective Immunity. J Immunol 207, 376–379 (2021).
14. Hajnik, R.L. *et al.* Dual spike and nucleocapsid mRNA vaccination confer protection against SARS-CoV-2 Omicron and Delta variants in preclinical models. Sci Transl Med 14, eabq1945 (2022).
15. Jia, Q. *et al.* Replicating bacterium-vectored vaccine expressing SARS-CoV-2 Membrane and Nucleocapsid proteins protects against severe COVID-19-like disease in hamsters. NPJ Vaccines 6, 47 (2021).
16. Chiuppesi, F. *et al.* Synthetic multiantigen MVA vaccine COH04S1 protects against SARS-CoV-2 in Syrian hamsters and non-human primates. NPJ Vaccines 7, 7 (2022).
17. Feng, W. *et al.* Nucleocapsid protein of SARS-CoV-2 is a potential target for developing new generation of vaccine. J Clin Lab Anal 36, e24479 (2022).
18. Dangi, T., Class, J., Palacio, N., Richner, J.M. & Penaloza MacMaster, P. Combining spike- and nucleocapsid-based vaccines improves distal control of SARS-CoV-2. Cell Rep 36, 109664 (2021).
19. Silva, E. *et al.* Immunization with SARS-CoV-2 Nucleocapsid protein triggers a pulmonary immune response in rats. PLoS One 17, e0268434 (2022).
20. Routhu, N.K. *et al.* A modified vaccinia Ankara vaccine expressing spike and nucleocapsid protects rhesus macaques against SARS-CoV-2 Delta infection. Sci Immunol 7, eabo0226 (2022).
21. McCafferty, S. *et al.* A dual-antigen self-amplifying RNA SARS-CoV-2 vaccine induces potent humoral and cellular immune responses and protects against SARS-CoV-2 variants through T cell-mediated immunity. Mol Ther 30, 2968–2983 (2022).
22. Chiuppesi, F. *et al.* Safety and immunogenicity of a synthetic multiantigen modified vaccinia virus Ankara-based COVID-19 vaccine (COH04S1): an open-label and randomised, phase 1 trial. Lancet Microbe 3, e252-e264 (2022).

23. Fleming, S.B., Wise, L.M. & Mercer, A.A. Molecular genetic analysis of orf virus: a poxvirus that has adapted to skin. Viruses 7, 1505–1539 (2015).
24. Rziha, H.J. *et al.* Parapoxviruses: potential alternative vectors for directing the immune response in permissive and non-permissive hosts. J Biotechnol 73, 235–242 (1999).
25. Buttner, M. & Rziha, H.J. Parapoxviruses: from the lesion to the viral genome. J Vet Med B Infect Dis Vet Public Health 49, 7–16 (2002).
26. Rziha, H.J. *et al.* Genomic Characterization of Orf Virus Strain D1701-V (Parapoxvirus) and Development of Novel Sites for Multiple Transgene Expression. *Viruses* 11 (2019).
27. Amann, R. *et al.* A new rabies vaccine based on a recombinant ORF virus (parapoxvirus) expressing the rabies virus glycoprotein. J Virol 87, 1618–1630 (2013).
28. Rohde, J., Amann, R. & Rziha, H.J. New Orf virus (Parapoxvirus) recombinant expressing H5 hemagglutinin protects mice against H5N1 and H1N1 influenza A virus. PLoS One 8, e83802 (2013).
29. van Rooij, E.M., Rijsewijk, F.A., Moonen-Leusen, H.W., Bianchi, A.T. & Rziha, H.J. Comparison of different prime-boost regimes with DNA and recombinant Orf virus based vaccines expressing glycoprotein D of pseudorabies virus in pigs. Vaccine 28, 1808–1813 (2010).
30. Henkel, M., Planz, O., Fischer, T., Stitz, L. & Rziha, H.J. Prevention of virus persistence and protection against immunopathology after Borna disease virus infection of the brain by a novel Orf virus recombinant. J Virol 79, 314–325 (2005).
31. Müller, M., Reguzova, A., Löffler, M.W. & Amann, R. Orf Virus-Based Vectors Preferentially Target Professional Antigen-Presenting Cells, Activate the STING Pathway and Induce Strong Antigen-Specific T Cell Responses. Front Immunol 13, 873351 (2022).
32. Reguzova, A., Ghosh, M., Müller, M., Rziha, H.J. & Amann, R. Orf Virus-Based Vaccine Vector D1701-V Induces Strong CD8 + T Cell Response against the Transgene but Not against ORFV-Derived Epitopes. Vaccines (Basel) 8 (2020).
33. Wu, F. *et al.* A new coronavirus associated with human respiratory disease in China. Nature 579, 265–269 (2020).
34. Wrapp, D. *et al.* Cryo-EM structure of the 2019-nCoV spike in the prefusion conformation. Science 367, 1260–1263 (2020).
35. Rizvi, Z.A. *et al.* Golden Syrian hamster as a model to study cardiovascular complications associated with SARS-CoV-2 infection. Elife 11 (2022).
36. Baden, L.R. *et al.* Efficacy and Safety of the mRNA-1273 SARS-CoV-2 Vaccine. N Engl J Med 384, 403–416 (2021).
37. Logunov, D.Y. *et al.* Safety and efficacy of an rAd26 and rAd5 vector-based heterologous prime-boost COVID-19 vaccine: an interim analysis of a randomised controlled phase 3 trial in Russia. Lancet 397, 671–681 (2021).
38. Polack, F.P. *et al.* Safety and Efficacy of the BNT162b2 mRNA Covid-19 Vaccine. N Engl J Med 383, 2603–2615 (2020).

39. Sadoff, J. *et al.* Safety and Efficacy of Single-Dose Ad26.COV2.S Vaccine against Covid-19. N Engl J Med 384, 2187–2201 (2021).
40. Voysey, M. *et al.* Safety and efficacy of the ChAdOx1 nCoV-19 vaccine (AZD1222) against SARS-CoV-2: an interim analysis of four randomised controlled trials in Brazil, South Africa, and the UK. Lancet 397, 99–111 (2021).
41. Heath, P.T. *et al.* Safety and Efficacy of NVX-CoV2373 Covid-19 Vaccine. N Engl J Med 385, 1172–1183 (2021).
42. Aydillo, T. *et al.* Immunological imprinting of the antibody response in COVID-19 patients. Nat Commun 12, 3781 (2021).
43. Rziha, H.J., Rohde, J. & Amann, R. Generation and Selection of Orf Virus (ORFV) Recombinants. Methods Mol Biol 1349, 177–200 (2016).
44. Caddy, S.L. *et al.* Viral nucleoprotein antibodies activate TRIM21 and induce T cell immunity. EMBO J 40, e106228 (2021).
45. Moss, P. The T cell immune response against SARS-CoV-2. Nat Immunol 23, 186–193 (2022).
46. Nelson, R.W. *et al.* SARS-CoV-2 epitope-specific CD4(+) memory T cell responses across COVID-19 disease severity and antibody durability. Sci Immunol 7, eabl9464 (2022).
47. Chan, J.F. *et al.* Simulation of the Clinical and Pathological Manifestations of Coronavirus Disease 2019 (COVID-19) in a Golden Syrian Hamster Model: Implications for Disease Pathogenesis and Transmissibility. Clin Infect Dis 71, 2428–2446 (2020).
48. L.J. REED, H.M. A SIMPLE METHOD OF ESTIMATING FIFTY PER CENT ENDPOINTS. American Journal of Epidemiology 27, 493–497 (1938).
49. Corman, V.M. *et al.* Detection of 2019 novel coronavirus (2019-nCoV) by real-time RT-PCR. Euro Surveill 25 (2020).
50. Wolfel, R. *et al.* Virological assessment of hospitalized patients with COVID-2019. Nature 581, 465–469 (2020).
51. Perera, R.A. *et al.* Serological assays for severe acute respiratory syndrome coronavirus 2 (SARS-CoV-2), March 2020. Euro Surveill 25 (2020).

Figures

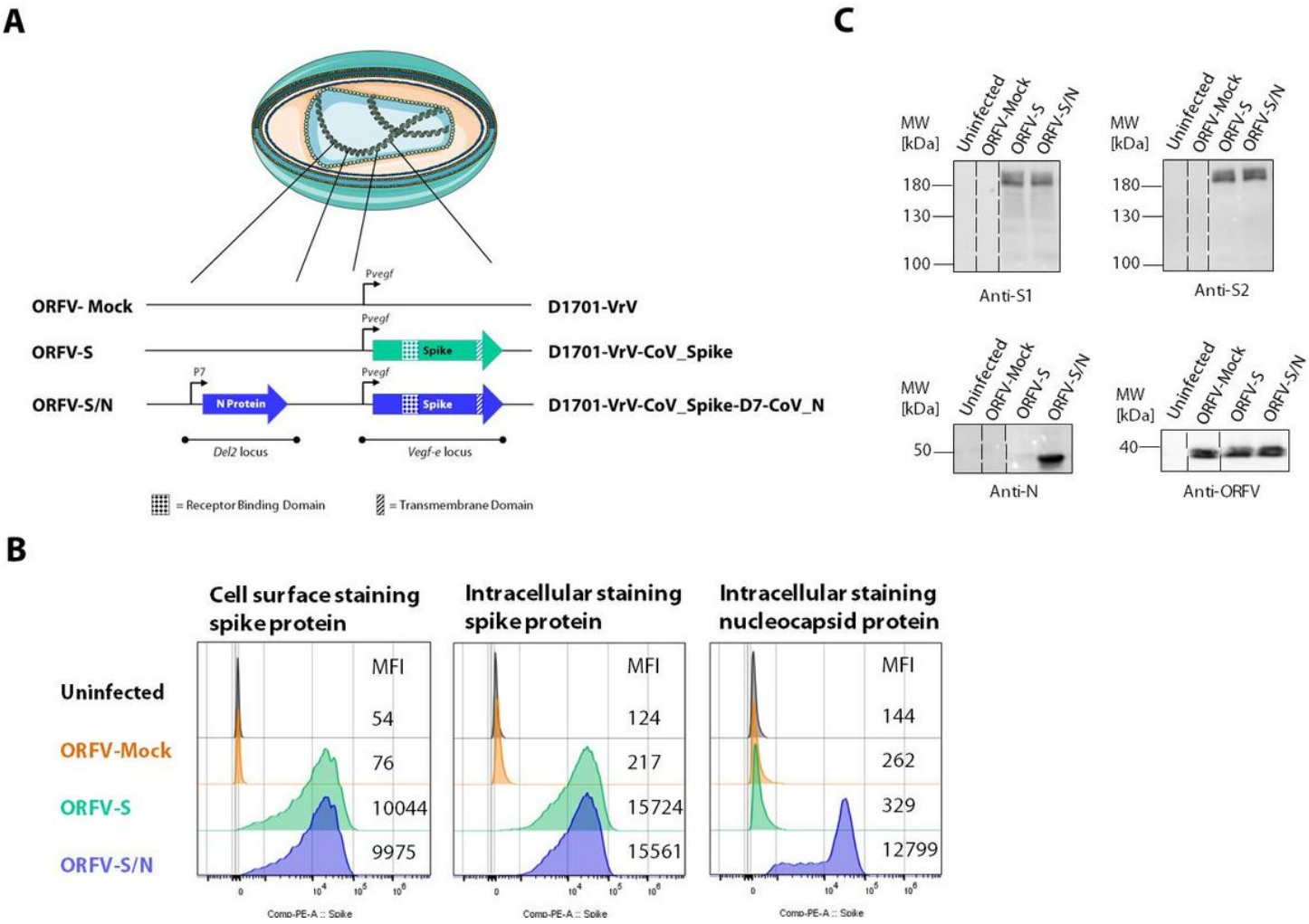

Figure 1

Construction and characterization of ORFV D1701-VrV-based SARS-CoV-2 recombinants. A) Scheme of D1701-VrV (ORFV-Mock), and D1701-VrV-CoV_Spike (ORFV-S) and D1701-VrV-CoV_Spike-D7-CoV_N (ORFV-S/N) ORFV recombinants. Spike gene was inserted at the *vegf-e* locus and expressed under the control of the natural *Pvegf* promotor. Nucleocapsid gene was integrated into the D (*Del2)* locus under the control of an artificial *P7*promotor. B) Flow cytometry analysis of Vero cells infected with the ORFV vectors for 20 h (MOI 1). Gated on spike and nucleocapsid protein expression was evaluated on the cell surface and intracellular using anti-S1, -S2, and -N antibodies, gating was done on ORFV-infected cells. Frequency of ORFV infected cells was approximately 20 % within each sample. Mean fluorescence intensity (MFI) is indicated for each sample. C) Western Blot analysis of Vero cells infected (MOI 1) for 48 h with the ORFV-S and ORFV-S/N. Antigen expression was evaluated using anti-S1, -S2, and -N antibodies in cell lysates. Broken lines indicate where the membrane was cut. Cells infected with ORFV-Mock or uninfected cells were used as controls as indicated.

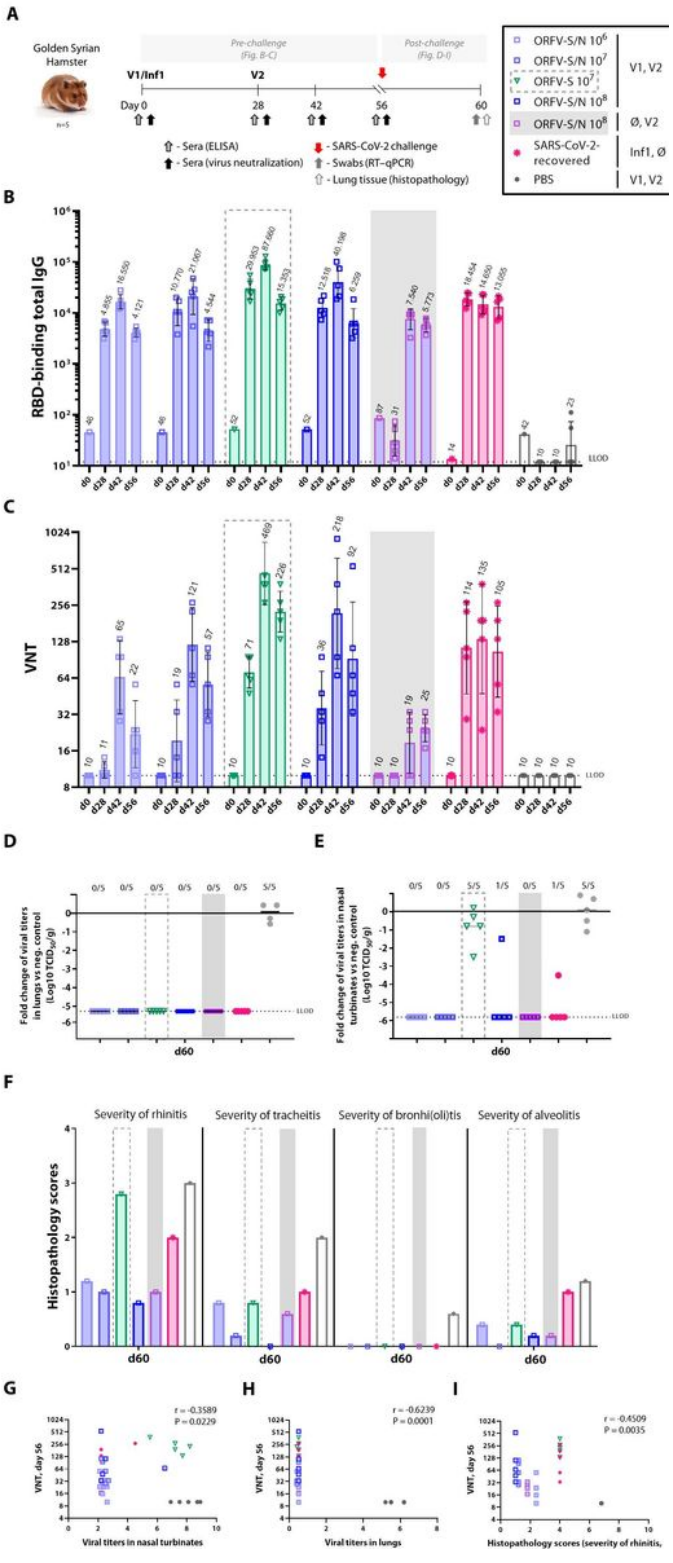
A
Golden Syrian Hamster
n=5
Pre-challenge (Fig. B-C)
Post-challenge (Fig. D-I)
V1/Inf1
V2
Day 0
28
42
56
60
⇧ - Sera (ELISA)
⬆ - Sera (virus neutralization)
⬇ - SARS-CoV-2 challenge
⇧ - Swabs (RT–qPCR)
⇧ - Lung tissue (histopathology)
ORFV-S/N 10^6
ORFV-S/N 10^7
ORFV-S 10^7
ORFV-S/N 10^8
ORFV-S/N 10^8
SARS-CoV-2-recovered
PBS
V1, V2
Ø, V2
Inf1, Ø
V1, V2
B
RBD-binding total IgG
LLOD
C
VNT
LLOD
D
Fold change of viral titers in lungs vs neg. control (Log10 TCID50/g)
LLOD
d60
E
Fold change of viral titers in nasal turbinates vs neg. control (Log10 TCID50/g)
LLOD
d60
F
Severity of rhinitis
Severity of tracheitis
Severity of bronhi(oli)tis
Severity of alveolitis
Histopathology scores
d60
G
r = -0.3589
P = 0.0229
VNT, day 56
Viral titers in nasal turbinates
H
r = -0.6239
P = 0.0001
VNT, day 56
Viral titers in lungs
I
r = -0.4509
P = 0.0035
VNT, day 56
Histopathology scores (severity of rhinitis,

Figure 2

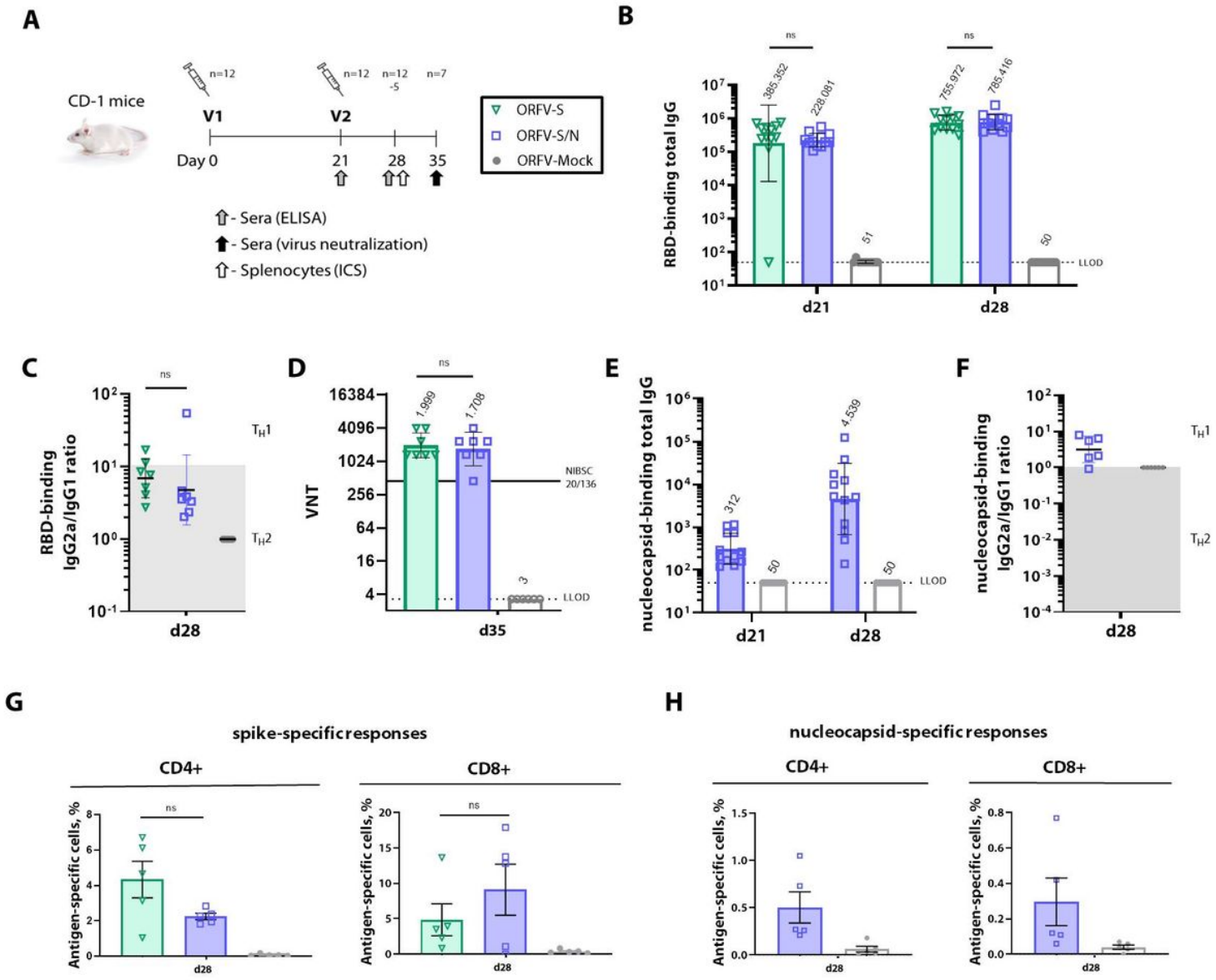

Figure 2

Immune responses stimulated by ORFV-S and ORFV-S/N recombinants in mice. A) CD-1 mice were immunized at day 0 (V1) and 21 (V2) with 10^7 PFU of ORFV-S and ORFV-S/N recombinants, or ORFV-Mock. B) RBD-specific total IgG endpoint titers in mouse serum, evaluated three weeks after the first (day 21) and one/ two weeks after the second (day 28/ day 35) immunization by ELISA. C) IgG2a/IgG1 isotype ratio of RBD-specific binding antibodies on day 28. D) SARS-CoV-2 (ancestral strain; Wuhan) serum virus neutralizing titer (VNT) on day 35. The horizontal solid line marks VNT in the WHO International Standard for anti-SARS-CoV-2 immunoglobulin NIBSC 20/136 reference panel. E) Endpoint titers of nucleocapsid-specific total IgG in mouse serum after the first (day 21) and second (day 28) immunization by ELISA. F) IgG2a/IgG1 isotype ratio of nucleocapsid-specific binding antibodies on day 28. Data are presented as geometric mean values ± geometric SD. G) Total percentage of spike- and H) nucleocapsid-specific CD4+ and CD8+ T cells producing IFNγ, TNF and IL-2 determined by flow

cytometry. Heights of bars indicate mean ±SEM. The dotted line indicates the lower limit of detection (LLOD). Geometric mean titers (GMT) are noted above each column.

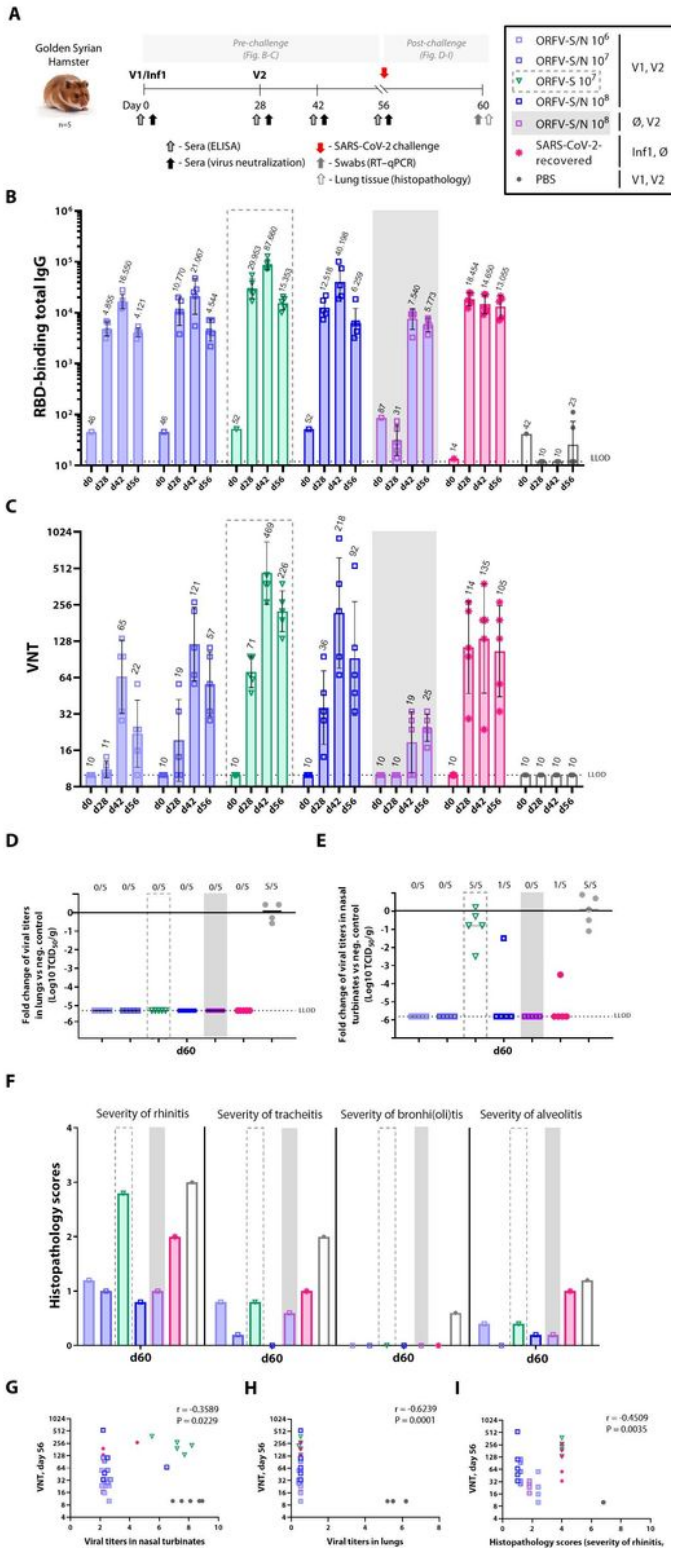

Figure 3

Protection against SARS-CoV-2 by vaccination with ORFV-S and ORFV-S/N recombinants in Syrian hamsters.

A) Hamsters were immunized with ORFV-S/N doses ranging from 10^6 to 10^8 PFU at days 0 (V1) and 28 (V2), or at day 28 only (V2) with 10^8 PFU, or with 10^7 PFU of ORFV-S for comparison. PBS was administered as negative control. As a reference, hamsters were inoculated intranasally with 10^2 $TCID_{50}$ SARS-CoV-2 (ancestral strain; Wuhan) on day 0 (Inf1) (SARS-CoV-2-recovered). All animals were challenged with 10^2 $TCID_{50}$ SARS-CoV-2 (ancestral strain; Wuhan) at day 56 and monitored for four days. B) Endpoint titers of RBD-specific total IgG in serum. C) Serum virus neutralizing titers (VNT) of SARS-CoV-2 (ancestral strain; Wuhan), solid line marks VNT in NIBSC 20/136 reference panel. Data are presented as geometric mean values ± geometric SD. Geometric mean titers are noted above the columns. Fold change of SARS-CoV-2 viral loads in D) lungs and E) nasal turbinates at day 60 normalized to Mock group. Data are presented as medians. Ratios above bars indicate the number of viral-RNA-positive animals per group. F) Histopathological analysis of tissues at day 60. Scoring was performed according to severity of inspected parameter; bars depict the median of each group. Spearman ´s correlation analysis of pre-challenge VNT with G) viral titers in nose, H) viral titers in lungs and I) histopathological scores at day 60. The dotted line indicates the lower limit of detection (LLOD).

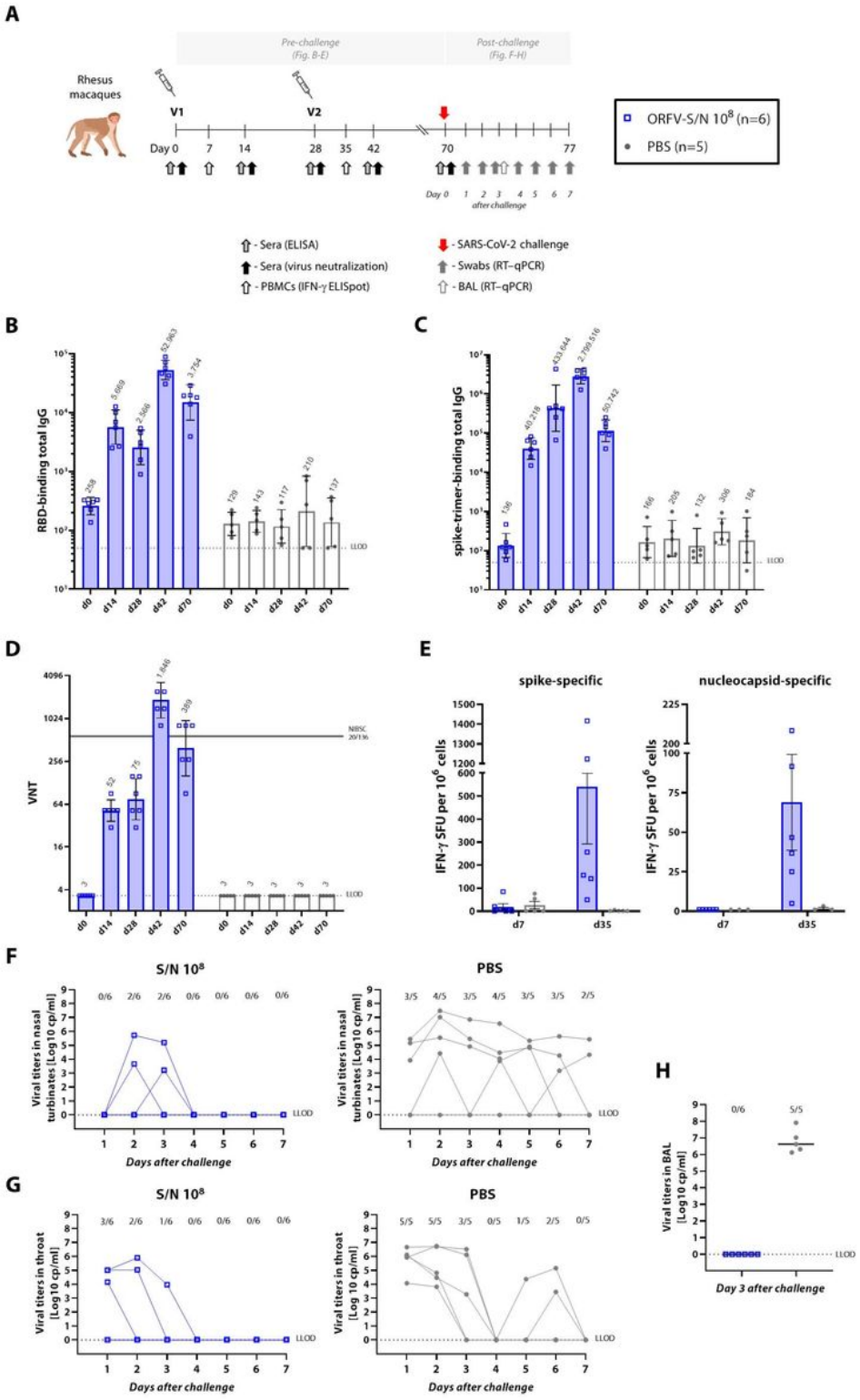

Figure 4

ORFV-S/N vaccine-induced protection in non-human primates (NHP). A) NHP were immunized twice with 10^8 PFU of ORFV-S/N recombinant, or PBS at days 0 and 28. All animals were challenged with 10^5 $TCID_{50}$ SARS-CoV-2, administered into nose and trachea at day 70 and monitored for the following seven days. Endpoint titers of B) RBD- and C) spike-trimer-specific total IgG in serum analyzed by ELISA. D) SARS-CoV-2 (ancestral strain; Wuhan) virus neutralizing titers (VNT) in serum. Solid line indicates VNT in

NIBSC 20/136 reference panel. Geometric mean titers are noted above the columns. E) IFNγ-secreting cells in PBMCs at day 7 and day 35 after 20 h stimulation with overlapping spike (upper graph) and nucleocapsid (lower graph) peptide pools, determined by ELISpot. SARS-CoV-2 viral loads in F) nose, G) throat and H) bronchoalveolar lavage (BAL) at indicated time points after challenge. Data are presented as medians. Ratios above bars denote number of viral RNA-positive macaques per group. The dotted line indicates the lower limit of detection (LLOD).

Supplementary Files

This is a list of supplementary files associated with this preprint. Click to download.

- FigS1.jpg
- FigS2.jpg
- FigS3.jpg
- FigS4.jpg
- Supplementarytables.docx